EVALUATION OF COSEISMIC LANDSLIDE HAZARD ON THE PROPOSED HAAST-HOLLYFORD HIGHWAY, SOUTH ISLAND, NEW ZEALAND

Tom R Robinson[1,2]*, Tim RH Davies[1], Thomas M Wilson[1], Caroline Orchiston[3], Nicolas Barth[4]

[1]Department of Geological Sciences, University of Canterbury, Christchurch, NZ

[2]Institute of Hazard, Risk, and Resilience, University of Durham, Durham, UK

[3]Department of Tourism, University of Otago, Dunedin, NZ

[4]Department of Earth Sciences, University of California, Riverside, USA

*corresponding author: tom.robinson@pg.canterbury.ac.nz

Abstract

Coseismic landsliding presents a major hazard to infrastructure in mountains during large earthquakes. This is particularly true for road networks, as historically coseismic landsliding has resulted in road losses larger than those due to ground shaking. Assessing the exposure of current and planned highway links to coseismic landsliding for future earthquake scenarios is therefore vital for disaster risk reduction. This study presents a method to evaluate the exposure of critical infrastructure to landsliding from scenario earthquakes from an underlying quantitative landslide hazard assessment. The method is applied to a proposed new highway link in South Island, New Zealand for a scenario Alpine Fault earthquake and compared to the current network. Exposure (*the likelihood of a network being affected by one or more landslides*) is evaluated from a regional-scale coseismic landslide hazard model and assessed on a relative basis from 0-1. The results show that the proposed Haast-Hollyford Highway (HHH) would be highly exposed to coseismic landsliding with at least 30-40 km likely to be badly affected (the Simonin Pass route being the worse

affected of the two routes). In the current South Island State Highway network, the HHH would be the link most exposed to landsliding and would increase total network exposure by 50-70% despite increasing the total road length by just 3%. The present work is intended to provide an effective method to assess coseismic landslide hazard of infrastructure in mountains with seismic hazard, and potentially identify mitigation options and critical network segments.

Keywords

Exposure analysis; hazard assessment; risk management; transportation networks; lifelines; Haast-Hollyford Highway; New Zealand

1. Introduction

Landsliding during earthquakes presents a major hazard and in some cases can cause as many impacts as, or more impacts than, the initial ground shaking. Recent disasters such as the 1999 Chi-Chi (Taiwan) and 2008 Wenchuan (China) earthquakes have vividly demonstrated this, with tens of thousands of landslides forming one of the most spatially extensive hazards (**Dadson et al., 2004; Gorum et al., 2011**). Evidence from previous earthquake disasters has shown that while building damage is the most common impact from ground shaking, damage and disruption to transport networks predominantly results from coseismic landsliding (**Bird and Bommer, 2004**). When planning new transport networks in mountainous regions with seismic hazard, it is therefore necessary to consider the exposure (herein defined as *the likelihood of being affected by a landslide)* of planned links to coseismic landsliding hazards (**Montibeller et al., 2006; Schroeder and Lambert, 2011**). One of the key elements in transport network planning is the identification of hazards which may impact proposed routes in the future using *scenario-based exposure analysis* (**Schroeder and Lambert, 2011; Goodwin and Wright, 2001; Montibeller et al., 2006**). The use of scenarios in transport planning has been shown to produce the information needed for decision-making (**Schoemaker, 1993**). Considering the exposure of planned transport links to potential future earthquake scenarios is therefore a useful and necessary step in sound decision-making. Nevertheless, difficulties in predicting potential coseismic landslide occurrence, runout, and volume amongst other things make coseismic landslide exposure modelling a difficult task. Developing an effective and globally applicable method to assess the exposure of critical infrastructure to landsliding from specific earthquake scenarios is therefore a vital research goal.

One such location where coseismic landslide exposure modelling is urgently required is the South Island of New Zealand, where large-scale rupture of the plate boundary Alpine Fault is considered to have a conditional probability of 28% in the next 50 years (**Biasi et al., 2015**). This fault accommodates ~80% of all Pacific-Australian plate boundary motion by coseismic slip (**Barth et al., 2014**), and is thought capable of producing M8 earthquakes (**Yetton, 1998; Sutherland et al., 2007; Berryman et al., 2012; Howarth et al., 2014**). Previous ruptures of this fault over the last 8 ka are thought to have resulted in widespread landsliding (**Howarth et al., 2012, 2014**) and empirical estimates suggest a future rupture could produce ~50,000 landslides (**Robinson and Davies, 2013**). Despite this, New Zealand's short recorded history (which began during European settlement c. 1840) means that only microseismicity (i.e. <M4) has been recorded on the Alpine Fault historically (**Boese et al., 2012**), and there are no sufficiently complete/accurate landslide inventories for other historic earthquakes in New Zealand. Consequently undertaking regional-scale coseismic landslide hazard assessments and subsequent exposure analyses for an Alpine Fault earthquake have not previously been possible. Recent advances however have enabled coseismic landslide hazard assessments in locations without historic inventories (**Kritikos et al., 2015**), further highlighting the need for a globally applicable exposure analysis method. The present work therefore develops a method to assess infrastructure exposure that can be applied to any coseismic landslide hazard model and applies it herein to a case study of a proposed highway in the South Island of New Zealand in the event of an Alpine Fault earthquake.

This proposed 150-160 km-long toll road (**Fig. 1**) would connect the popular tourist destinations of Milford Sound and south Westland via existing road ends in the Hollyford and Cascade River valleys (**Otago Daily Times, 2015**). The new link road, known as the Haast-Hollyford Highway (HHH), is intended to provide easier access between the West Coast region and Milford Sound by reducing the current journey distance by ~355 km, saving four to five hours driving time (**The Press, 2014; Wilderness Magazine, 2014**), as well as creating tourist access to natural areas of high scenic value (including remote areas of Fiordland National Park, Mount Aspiring National Park, Olivine Wilderness Area, and Te Wāhipounamu-South West New Zealand UNESCO World Heritage Area). The road is expected to be used by >900,000 people in its first year and construction costs have been estimated at NZ$220-250 million, although other independent estimates suggest this could exceed NZ$1 billion (**Otago Daily Times, 2014, 2015**). The HHH route passes through steep terrain in which multiple prehistoric large (>1 million m^3) landslides have been identified (**Fig. 1**), including some tentatively attributed to earthquake shaking (see **Barth, 2013a**). The majority of the proposed route for the HHH is within 10 km of the Alpine Fault, suggesting it may be highly exposed to landsliding in a future earthquake on this fault. Assessing the exposure of the HHH to landsliding during an Alpine Fault earthquake is therefore urgently required in order to inform decision-making with regards to planning for the road.

The present work is intended to demonstrate the value of assessing exposure to coseismic landsliding for the purposes of aiding decision-making, and to illustrate a method for the analysis of existing and planned transport links in mountainous regions with seismic hazards.

2. Background

2.1 Haast-Hollyford Highway

A route connecting Haast to several locations via the Cascade and Hollyford Rivers has been considered several times since the 1870s (**Archives New Zealand, 2015**; **The New Zealand Herald, 2010; Otago Daily Times, 2014**). In 1884 a topographical plan was published (**Archives New Zealand, 2015)** showing a proposed road between Jackson Bay and Lake Wakatipu, whose route followed the Cascade, Pyke, and Hollyford Rivers via Simonin Pass (**Fig. 1**). Two years later an alternative route was proposed through the same area crossing the Gorge River (**Fig. 1**), although this did not appear on official maps until 1966 (**New Zealand Map Series 10, 1966**). Some construction work occurred in the 1890s (**The New Zealand Herald, 2010**), but no road suitable for vehicular access has ever been completed south of the Cascade River (**Fig. 1**). It seems most likely that any road constructed here will follow the Gorge River route, which was assessed by Environment Southland in 2012 (**Oldfield, 2012**), however some reports still suggest the 1884 Simonin Pass route may be used (see **The Press, 2014**). Construction would involve upgrading ~70 km of existing road southwest of Haast and along the Hollyford River, in conjunction with building 80-90 km of new road between the existing road ends, giving a total road length of 150-160 km (**Fig. 1**).

2.2 Alpine Fault earthquake hazard

The Alpine Fault is a >400 km long, seismic, dextral-oblique plate boundary fault between the Pacific and Indo-Australian tectonic plates (**Berryman et al., 1992**). Pre-historic earthquakes on the fault have been estimated to be M_w8.0+ from a combination of on- and off-fault data (**Yetton, 1998**; **Wells et al., 1999**; **Howarth et al., 2012, 2014**; **De Pascale and Langridge, 2012**). Over the last 8 ka the Alpine Fault has had a relatively invariable average earthquake recurrence interval of 329±68 years, with the last event dating to 1717 CE, prior to European settlement (**Berryman et al., 2012**). Recent damaging earthquakes in the South Island have therefore primarily occurred on subsidiary faults with recurrence intervals >1000 years compared to the ~300 years for the Alpine Fault. Historical earthquakes on the Alpine Fault have been confined to relatively minor (i.e. <M4)

earthquakes (Boese et al., 2012), causing no damage and no recorded landsliding. Large, pre-historic earthquakes on this fault are known to have occurred however, and are thought to have resulted in widespread geomorphic consequences, most notably in the form of landsliding (**Yetton, 1998; Wells et al., 1999; Wells and Goff, 2007; Howarth et al., 2012, 2014**). An initial assessment of the potential scale of landsliding likely to arise from a M_w8.0 Alpine Fault earthquake was presented by **Robinson and Davies (2013)**, who suggested that several tens of thousands of landslides could affect >30,000 km^2 of the South Island.

More than 50 large (>1 million m^3) pre-historic landslides have been identified in the region between Haast and Milford Sound (**Fig. 1**), three of which are among the five largest landslides identified in New Zealand. Given their proximity to the Alpine Fault, the majority of these are thought to have occurred during previous Alpine Fault earthquakes (**Korup, 2004; Hancox and Perrin, 2009; Barth, 2013a**). Both routes for the HHH cross the 0.75 km^3 Cascade rock avalanche deposit; **Barth (2013a)** identified a prominent *sackung* (a scarp indicative of slow, deep-seated gravitational deformation) contiguous to its head-scarp, suggesting that there was potential for a further 0.25 km^3 failure towards the proposed road. The proximity of both HHH routes to the Alpine Fault, as well as the steep terrain and number of identified landslide deposits in the region, suggests there is likely to be a high coseismic landslide hazard. Determining the exposure of the HHH to landsliding during an Alpine Fault earthquake is therefore relevant in the context of the proposal to develop the HHH.

2.2.1 An Alpine Fault earthquake scenario

Using a variety of different methods, including fault trenching, tree coring, landscape offset features and others, a number of studies have concluded that the Alpine Fault produces characteristic (i.e. unimodal) earthquakes, many of which have been demonstrated to involve rupture of ~380 km of the fault between Milford Sound and the Ahaura River (**Berryman et al., 2012; De Pascale and Langridge, 2012; Howarth et al., 2014; Leitner**

et al., 2001; Wells and Goff, 2007; Wells et al., 1999). As stated above, these correspond to ~M_w8.0 earthquakes. No evidence of rupture along the Alpine Fault has been identified post-1717 CE, which, in combination with measured plate motions, suggests the next rupture could involve horizontal displacements of >7 m and a magnitude ~M_w8.0. The scenario considered herein therefore involves a M_w8.0 earthquake with ~380 km fault rupture between Milford Sound and the Ahaura River.

Shaking intensity in the form of Modified Mercalli (MM) intensity is simulated using open source earthquake hazard analysis software OpenSHA, which calculates the probability that an Intensity Measure Type (IMT) will exceed some Intensity Measure Level (IML) (**Field et al., 2003**). Using data derived from the literature and presented in **Table 1**, OpenSHA is used to model the shaking intensity with a 50% exceedance probability (this is the default modelling parameter for MM intensity in OpenSHA (**Field et al., 2003**)). The resulting earthquake scenario is shown in **Figure 2**.

3. Methods

3.1 Exposure analysis

Landslide risk assessments are a complex task due to the difficulty in predicting landslide occurrence, runout length and direction, debris volume etc. Recent attempts have therefore focussed on evaluating exposure as a function of landslide hazard (**Pellicani et al., 2014; Catani et al., 2005**). Landslide hazard models can be either quantitative or qualitative, but both assess the likelihood of a landslide occurring at any given location throughout the study region from a particular scenario. To do this they utilise raster data in Geographic Information Systems (GIS), with each cell in the raster layer describing the modelled hazard corresponding to its location. In quantitative assessments, the models describe the hazard in terms of either absolute or relative likelihood of a landslide occurring on a scale of 0-1 (or 0-100%), with each individual cell taking a unique value in this range (e.g. **Kritikos et al., 2015**). Using quantitative hazard assessments allows exposure to also be modelled quantitatively, and thus effectively measures *the relative or absolute likelihood from 0-1 of the asset being affected by one or more landslides*, where 1 is almost certain (in the case of relative likelihood) and 0 is (almost) never as defined in probability theory. Such approaches are preferred to qualitative analyses (which present exposure descriptively as ‘very high’, ‘very low’, ‘medium’ etc.) as they provide empirical data which can be analysed and compared to other locations, networks, and/or hazards. The method proposed herein therefore focusses on determining coseismic landslide exposure from any underlying quantitative coseismic landslide hazard model.

In full risk assessments, such as those in **Catani et al. (2005)** and **Pellicani et al. (2013)**, risk metrics such as monetary loss are measured in order to establish the total risk posed to the network. In order to keep the method herein generally applicable, such risk metrics are not defined; instead exposure focuses solely on the likelihood of the network being affected. This is undertaken because estimated construction costs for proposed infrastructure links can vary substantially (e.g. for the HHH they vary by nearly an order of magnitude: NZ$200 million to 1 billion; **Otago Daily Times, 2014, 2015**), making risk metrics difficult to develop. Nevertheless, the definition and measure of exposure herein provides information that may be critical in route selection and design, whilst allowing the subsequent inclusion of risk metrics such as monetary loss if desired.

To model network exposure from a landslide hazard model, the method must consider not only the likelihood of a landslide occurring, but also its potential to affect the network should it occur. This requires potential landslide runout length and direction to be considered as these factors dictate the area a landslide will affect. Combining runout length and direction therefore defines an area surrounding a network within which any landslide that occurs has the potential to affect the network. In the underlying landslide hazard model, the cells included within this area describe the likelihood of a landslide occurring in each cell, and can thus be used to describe the corresponding exposure. In order to ensure that the cells involved are appropriate i) the cells must be within a maximum specified distance of the network, and ii) the cells must occur in areas where landslide runout has potential to affect the network. The former prevents cells requiring unreasonably large runout distances to affect the network from being incorporated, while the latter precludes incorporating cells within the defined proximity but on slopes facing away from the road (**Fig. 3**).

Horizon lines (also known as ridgelines) are established at equal intervals along the network using GIS (**Fig. 3**). Horizon lines identify the visible horizon for an observer positioned at a defined point on the earth's surface and can be limited to show the horizon at any desired distance (i.e. the maximum considered runout distance, see below). This therefore identifies the region within which any landslide that occurs has the potential to impact the observer, assuming landslide runout is in the steepest downhill direction. Thus it can be used to define the area around any point on a network within which the hazard values of all cells will be evaluated (**Fig. 3**).

Maximum likely runout distance can be set by the user to represent the maximum distance considered plausible. This distance should be carefully selected so as to avoid ignoring the potential for long-runout landslides, while not overestimating exposure by including cells requiring unreasonably large runout distances to impact the network. It is suggested herein that a maximum runout distance of 1 km be used. Various studies have used empirical calculations to link landslide volume to maximum runout distance (e.g. **Davies, 1982; Hungr et al., 2005; Kilburn and Sorenson, 1998; Legros, 2002; Nicoletti and Sorriso-Valvo, 1991; Scheidegger, 1973**) and each of these suggests that a runout of 1 km requires a landslide volume of at least 1 million m^3. **Brunetti et al. (2009)** and **Stark and Guzzetti (2009)** assessed a global compilation of landslides from all triggers in order to identify their volume distribution, and found the probability of any given landslide having a volume greater than 1 million m^3 is $<10^{-7}$ (1 in 10 million). While volume is not the only factor affecting runout (water content can increase runout distance for instance), this suggests the likelihood of runout distances >1 km is similarly unlikely. Considering distances larger than 1 km without evidence such events are common in the study region therefore risks overestimating the exposure of the network by over-emphasising the possibility for landslides >1 million m^3. For instance, larger-volume landslides have occurred multiple times historically in New Zealand, and there are particularly large numbers of pre-historic examples in the HHH region (**Fig. 1**) suggesting such landslides may be more common here. Nevertheless the likelihood of a landslide >1 million m^3 occurring at any given location in the next Alpine Fault event is very small, and thus is not considered for exposure modelling.

Consequently, coseismic landslide exposure is derived from the mean hazard values of all cells within a 1 km horizon line of any given point on the network (**Fig. 3**). In order to deal with issues arising from using discrete points on a continuous network, points are selected at a user defined distance (herein every 500 m) along the network and exposures are interpolated between these using the inverse distance weighting (IDW) method within ESRI's Arc GIS (see **ESRI, 2015a**). The mean value of surrounding cells is used as this best represents the total exposure of the network. Using the maximum hazard cell would represent the highest likelihood of a landslide occurring in the considered region; however this does not necessarily accurately represent the likelihood of a network being affected by a landslide. For instance, consider two sections of the same network; one surrounded by mountains with high hazard on all sides and one along the range-front with mountains with similarly high hazard on one side and flat plains with low hazard on the other. Using the highest observed hazard would suggest both sections are similarly exposed (**Fig. 4**), however this ignores the fact that the section within the mountains can potentially be impacted from all sides while the range-front section can only be affected from one side. Using mean cell values accounts for this by considering the low hazard cells also present around the range-front section, thus correctly identifying this section as being less exposed (**Fig. 4**).

3.2 Coseismic landslide hazard assessment

In order to assess the exposure of the HHH, an underlying quantitative coseismic landslide hazard assessment for an Alpine Fault earthquake is required. Such assessments have not previously been possible in New Zealand due to a lack of accurate historic coseismic landslide inventories (i.e. compiled via GIS from aerial/satellite photography) and adequate geotechnical data. However, **Kritikos et al. (2015)** have developed a method to assess the coseismic landslide hazard resulting from a specific earthquake scenario despite a lack of accurate historical and geotechnical data. They showed that such an analysis could be undertaken via fuzzy logic in GIS by evaluating historic coseismic landslide inventories from several different locations. **Kritikos et al. (2015)** demonstrated that combining data from landslide inventories for the 1994 Northridge and 2008 Wenchuan earthquakes could accurately predict the spatial distribution of coseismic landslide hazard during the 1999 Chi-Chi earthquake, using only earthquake-rupture parameters and a digital elevation model (DEM).

To model coseismic landslide hazard for scenario earthquakes, **Kritikos et al. (2015)** established the effect of various pre-disposing factors on landslide occurrence in the 1994 Northridge and 2008 Wenchuan earthquakes. They found that changes in MM intensity, slope angle, proximity to mapped active faults and streams, and slope position had similar effects on landslide occurrence in both events. As slope angle increased from <5°, the rate of landsliding increased dramatically across both environments, with the highest rate of landsliding occurring on slopes >45°. Slope position was assessed with regards to ridgelines, mid-slopes, valleys, and flat ground, with dramatic increases in the rate of landsliding at ridgetops compared to other slope positions, highlighting the importance of topographic amplification (**Kritikos et al., 2015**). Slopes in close proximity (i.e. <~1 km) to active faults and stream systems were also found to have a higher rate of landsliding, likely due to increased erosion weakening the rock mass. Finally, landslide density was seen to increase with MM intensity, with a minimum required intensity of MM5 in accordance with observations elsewhere (**Keefer, 1984**).

These relationships were therefore modelled and combined using fuzzy logic in GIS, under the assumption that similar relationships occur in other environments, such as Taiwan and New Zealand. The resulting output is a map describing the relative probability of landslide occurrence from 0 to 1 on a cell-by-cell basis for the given earthquake scenario. When applied to the 1999 Chi-Chi earthquake, this model achieved >90% success rate despite using relationships derived from different earthquake scenarios (**Kritikos et al., 2015**). This suggests that the relationships identified in China and California are also applicable to Taiwan, with effects like topographic amplification and slope angle having similar influence on the rate of landsliding. The Chi-Chi earthquake shares many similarities with an anticipated Alpine Fault earthquake in that it involved oblique slip along a range-front fault (**Chi et al., 2001**), occurred in a region with relatively high seismicity and rapid plate motions (**Yu et al., 1997**), and affected heavily vegetated and weathered mountains comprising primarily of schist (**Zhang and He, 2002**). Further, **Robinson (2014)** showed that the **Kritikos et al., (2015)** method achieved suitable results for two historic New Zealand earthquakes. This suggests this method can be applied to an Alpine Fault scenario under the assumption that similar accuracy for the spatial distribution of landsliding to that for Chi-Chi can be achieved.

To apply the method of **Kritikos et al. (2015)** an earthquake scenario in terms of MM Intensity is required along with the spatial distribution of slope angle, proximity to faults and streams, and slope position within the study region. MM Intensity is shown in **Figure 2** and the remaining factors are derived from a 60x60 m cell size South Island DEM (sampled from Land Information New Zealand's (LINZ) 20 m DEM), and the New Zealand Active Fault Database (http://data.gns.cri.nz/af/). A 60 m DEM is used as this provided **Kritikos et al. (2015)** the finest DEM resolution available for all study regions that exceeded the landslide inventory mapping accuracy. Stream systems are defined using the Flow Accumulation tool within ESRI's Arc GIS (**ESRI, 2015b**) with a catchment area of 1 km^2 required to form a stream. Mapped active faults are defined as those faults included in the GNS Science active fault database (http://data.gns.cri.nz/af/) and those in **Barth et al. (2013)**.

4. Application to the Haast-Hollyford Highway

The relative coseismic landslide hazard for the study region is shown in **Figure 5**. This map is characterised by high hazard values (i.e. close to 1) in the steep terrain close to the Alpine Fault, with a maximum relative hazard of 0.97 and a minimum of 0.22. In total, 421 km^2 (~5%) of the study area has relative hazard >0.9 and 2000 km^2 (~25%) >0.75; the mean hazard value across the entire area is 0.64. This corresponds well with geologic observations suggesting this region has a high coseismic landslide hazard and is therefore likely to experience widespread and extensive landsliding during an Alpine Fault earthquake, as occurred in the Chi-Chi and Wenchuan earthquakes.

It is important to note that the hazard values involved describe *relative hazard* rather than *absolute hazard*, with the value in any specific cell giving the probability of landslide occurrence *relative to all other cells in the study area*. A value of 1 therefore indicates a cell that, relative to all other cells, is *almost certain* to produce a landslide. If this were absolute hazard, a value of 1 would represent a cell *certain* to produce a landslide regardless of the values in other cells. Also, because this model describes hazard (i.e. likelihood of occurrence), a landslide can plausibly occur at any value between 0 and 1, but is inherently more likely to occur in cells where values are closer to 1.

The consequent exposure map for the HHH is shown in **Figure 6**. This shows that both the Gorge River and Simonin Pass routes have long sections with large exposure values. The highest observed exposure on the Gorge River route is 0.88, which occurs close to the northern intersection of both proposed routes (**Fig. 6**). In total, ~31 km (~20%) of the Gorge River route has exposure values >0.75, of which only a third is on the existing section of the route (**Fig. 6**). The highest observed exposure on the Simonin Pass route is 0.89, which occurs ~15 km south of the northern intersection of the proposed routes (**Fig. 6**). In total,

~40 km (~25%) of the Simonin Pass route has exposure values >0.75, again only a third of which is on the existing sections of road (**Fig. 6**). Despite the largest observed exposure values being confined to the middle 20-25% of the routes, exposures of ~0.7 are observed on multiple sections south of Big Bay (**Fig. 6**).

Applying the exposure analysis method to the entire South Island State Highway (SH) network for the same earthquake scenario (**Fig. 7**) allows a comparison to be made between the proposed HHH and the existing network. The highest observed exposure on the current network is 0.87 between Franz Josef and Fox Glacier (**Fig. 7**), which is lower than the maximum observed on both proposed HHH routes. In total, only 55 km (~1%) of the current SH network (>5000 km) has exposure values >0.75. The HHH would increase this by 56-72% while increasing the total network length by just ~3%. Currently, the longest continuous section of the network with exposure >0.75 is a 13 km section through Arthur's Pass (**Fig. 7**), which is already widely acknowledged as being at extreme risk to damage/disruption from both coseismic and aseismic hazards (**Paterson, 1996**); however this is only half that of the longest similarly exposed sections of both HHH routes. It appears the HHH would be the highway most exposed to coseismic landsliding during an Alpine Fault earthquake, and would substantially increase the exposure of the entire South Island State Highway network.

5. Discussion

5.1 Implications for the Haast-Hollyford Highway proposal

This study has demonstrated that the HHH would have an extremely high exposure to landsliding during an Alpine Fault earthquake. Much of the South Island's State Highway network was built before the earthquake hazard from the Alpine Fault was fully understood. Consequently, highway links such as Arthur's Pass and SH6 along the west coast have only subsequently been accepted as being at extremely high risk to disruption during an earthquake (e.g. **Paterson, 1996**). The HHH would present a substantially higher risk than both of these highways and thus would most likely be the worst-affected highway on the network following an Alpine Fault earthquake. Given the length of road exposed to landsliding along the HHH, it is likely that similar levels of restoration would be required for the HHH post-earthquake as for the whole of the current network. In order to significantly reduce the exposure of the proposed routes, substantial engineering techniques such as tunnelling would need to be undertaken during the initial road construction. Such methods are likely to dramatically increase the initial construction costs of the HHH, which have already been estimated at up to NZ$1 billion, and thus may not be viable.

Acceptable risk in terms of life-safety has not been estimated herein as absolute hazard has not been calculated. Nevertheless, consideration should be given to the potential risk to future road users, as well as to construction workers should an earthquake occur during construction. Any person in the vicinity of the HHH during an Alpine Fault earthquake would likely be the most exposed to landsliding of anyone on the South Island State Highway network. Given the suggested popularity of the road, development of further infrastructure along the HHH, particularly petrol stations, look-outs/viewing points, picnic facilities etc., is also likely, placing the facilities and their users at risk.

5.2 Other hazards

Although the Alpine Fault is the major tectonic feature and the source of the main seismic hazard in the South Island (**Stirling et al., 2012**), other faults are known to exist in its vicinity (**GNS Active Faults database**; http://data.gns.cri.nz/af/; Fig. 1 of **Barth et al., 2013**) and there are a number of faults in the area with unknown seismic hazard. Of particular note is the Puysegur subduction zone whose northernmost extent is directly offshore from the proposed HHH (**Barnes et al., 2005**). The Puysegur subduction zone is thought to be the source of the 1826 CE Fiordland earthquake which generated a tsunami at Okarito (>200 km north of HHH) and triggered widespread geomorphic effects in south Westland including landslides, forest disturbances, and coastal dune formation (**Barnes et al., 2013; Goff et al., 2004; Wells et al., 2001; Wells & Goff, 2007**). In the George Basin 35 km southwest of

Milford Sound, **Barnes et al. (2013)** determined a mean recurrence interval of 191 years for large magnitude paleo-earthquakes assumed to be associated with the Alpine Fault and the Puysegur subduction zone; this is a shorter recurrence interval than the 329±68 years estimated for the Alpine Fault 20 km north of Milford Sound (**Berryman et al. 2012**), suggesting that major Puysegur trench earthquakes are also a significant hazard to the HHH region.

Several studies have shown that an Alpine Fault earthquake is likely to generate a wide range of cascading geomorphic hazards as well as seismic hazards, most of which have not been considered herein (**Robinson and Davies, 2013; Yetton, 1998; McCahon et al., 2006**). Given the HHH's proximity to the Alpine Fault, in addition to landsliding the road is likely to be exposed to surface rupture, strong ground shaking, lateral spreading, debris flows, and long-term river aggradation hazards. **Barth et al. (2014)** undertook detailed investigations of slip rates along the Alpine Fault in this region and concluded that single event displacements here are likely to exceed 10 m horizontally. In an Alpine Fault earthquake, multiple instances of very large surface displacements, potentially similar to the road width, are therefore expected on the HHH. The route also requires large new bridges across the Pyke and Cascade Rivers (**Otago Daily Times, 2014**) as well as numerous smaller new bridges and upgrades to existing bridges, particularly across the Arawhata River (**Fig. 1**). In an Alpine Fault earthquake these bridges would be exposed to MM 8-9 shaking (**Fig. 2**) and would be unlikely to survive unless specifically designed and constructed to withstand such shaking. Lateral spreading of bridge abutments is also likely, as was witnessed in Christchurch during the Canterbury earthquake sequence (**Giovinazzi et al 2011**) when similar shaking intensities occurred, but for a shorter duration.

Finally, following the earthquake, sediments deposited on slopes and in valleys by landsliding will be remobilised by debris flows and fluvial processes during the heavy rainstorms common in the region. Following the 2008 Wenchuan earthquake, heavy and long-duration rainstorms reactivated landslide material as highly mobile debris flows that buried downstream areas (including townships) by up to ~5 m (**Xu et al., 2012**). Annual rainfall in the HHH region exceeds 10,000 mm on average with maximum daily rainfall >300 mm (**England, 2011**). Combined with the modelled landslide hazard this suggests that post-earthquake debris flows are likely to pose a further hazard to the highway. Further, **Howarth et al. (2012, 2014)** showed that sediment remobilisation and deposition following Alpine Fault earthquakes was extensive and could continue for several decades, raising river beds by up to several metres. Consequently, large sections of the road may become exposed to long-term flooding hazards and channel avulsion may result in some rivers changing course and occupying the road.

5.3 Implications for infrastructure exposure modelling

The method described herein has been shown to be able to assess the exposure of infrastructure links from coseismic landslide hazard assessments for scenario earthquakes. This may allow greater understanding of the risk posed from future anticipated earthquakes in regions where current understanding has previously been limited. The method is applicable to both current and planned infrastructure links, and can therefore be used to plan post-event emergency response options as well as inform route planning/selection. It may also allow the identification of critical network segments where mitigation measures can be focussed in order to increase resilience and reduce losses. Herein, this method has been applied on a deterministic basis, however its reliance on only an underlying coseismic landslide hazard model may allow for probabilistic risk assessment to be undertaken assuming a probabilistic landslide hazard model is available or can be developed.

This work has also demonstrated the usefulness of first-order exposure analyses for hazard and risk analysis and subsequent planning when presented with a lack of empirical data. Despite a lack of data, such approaches can allow initial hazard assessments (including in rapid post-earthquake responses) to which more focussed and detailed studies can subsequently add. The results herein have shown that the HHH is substantially exposed to an M8 Alpine Fault earthquake; however other seismic scenarios are possible for the Alpine Fault and earthquakes on other faults are also likely (see above). This analysis has therefore highlighted the need for further study into the exposure of the HHH to all seismic threats and it is suggested that future work investigate the exposure both to alternative shaking scenarios as well as on a probabilistic basis using the National Probabilistic Seismic Hazard model of **Stirling et al. (2012)**. Undertaking assessments such as that presented herein for regions where empirical data is limited or lacking entirely is likely to yield similar benefits with regards to hazard and risk assessments and disaster risk reduction/management.

5.4 Modelling limitations

The modelling approach undertaken in this study has assumed that landslide runout occurs in the steepest downhill direction. In some instances however, landslides can have complex runout paths by becoming channelized within narrow valley systems (see **Okada et al., 2008**), fluidised during heavy rainfall (**Legros, 2002**), or simply as a result of extremely large volumes (e.g. **Huang et al., 2012; Robinson et al., 2014**). **Chevalier et al. (2009)** showed that the coseismic Mt Wilberg rock avalanche in Westland, New Zealand ran out at right angles to the fall line and parallel to the Alpine Fault. Thus there is the potential for the HHH to be exposed to further landslide hazards beyond the 1 km maximum distance considered herein. Such complex runout paths are unlikely however, and modelling runout paths for potentially hundreds-to-thousands of landslides when their precise locations and behaviour are unknown is not feasible. Nevertheless, this uncertainty should be considered when interpreting the results.

Consideration should also be given to the fact that not all landslides occurring within the 1 km limit will affect the road. Small volume landslides in particular will likely have runout paths <<1 km and thus if they were to occur several hundred metres from the road, may not affect it. Since we have used the same methodology for all South Island highways however, the exposure of the HHH relative to these remains valid.

A further point to consider is the occurrence of landslides larger than 1 million m^3. **Figure 1** shows at least 50 of these landslides occurring in the study area since the last deglaciation at ~ 18 ka, and **Dykstra (2012)** identified more than 20 further deposits beneath Milford Sound. Such landslides can have runouts far larger than 1 km (e.g. **Hsü, 1975**), and could therefore affect the road even if they occur at distances greater than that considered herein. The 1.1 billion m^3 Daguangbao landslide that occurred during the 2008 Wenchuan earthquake ran over the ridgeline opposite the headscarp, affecting the adjacent valley (**Huang et al., 2012**). Nevertheless, anticipating whether and where such large landslides will occur in future scenarios is a difficult task that cannot realistically be incorporated into a regional hazard assessment such as this, and again the relative exposure of the HHH compared to other highways remains valid.

Uncertainties within the initial coseismic landslide hazard modelling should also be considered. These are primarily based around the cell size used during the modelling. The hazard values for each cell are a direct result of the values of each pre-disposing factor in the corresponding cell. When considering factors such as slope angle, larger cell sizes will produce less accurate slope angles compared to smaller cell sizes. Consequently, the resulting hazard value will be equally inaccurate. Nevertheless, using cell sizes smaller than the initial landslide inventory accuracy can result in landslides being associated with incorrect cells, thus providing incorrect results as to the influence of each pre-disposing factor on landslide occurrence. **Kritikos et al. (2015)** therefore elected to use 60x60 m cell size DEMs as this provided the smallest cell size available for all study regions that was larger than the accuracy of the landslide inventories involved.

Further, the effect of geology is not directly considered in the **Kritikos et al. (2015)** method. Nevertheless, several topographic factors are considered, which suggests that the effect of geology is at least partially considered as topography is partly controlled by the underlying geology. For instance the differences between the Southern Alps and Fiordland are partially controlled by the change from schist in the Southern Alps to granite in Fiordland. **Kritikos et**

al. (2015) did show however that geology was not required to sufficiently estimate the spatial distribution of coseismic landslide hazard by achieving successful results without including the effect of geology. Instead they suggested that geology may affect the rate of landsliding that occurs (i.e. control the value above which landsliding is more likely) rather than the spatial distribution of hazard, which is instead controlled by shaking intensity and topography. Nonetheless, if information on the effect of geology in a study region is known, particularly with respect to the type of landslide and potential volume, this can be included both in the underlying coseismic landslide hazard model and in the selection of maximum runout distance during exposure modelling. Such data therefore has the potential to provide a more detailed and robust exposure analysis.

Lastly, it should be highlighted that the approach herein has focussed on the use of MM intensity as the measurement for the triggering mechansim (ground shaking). Other measurements, such as Arias intensity, PGA, or PGV have also been widely used for the modelling of landslide hazard however (**Lee, 2014; Jibson, 2007; Chousianits et al., 2014**). In the absence of strong motion data, as is typically the case for future scenario earthquakes, the use of MM intensity to measure ground shaking is more common as it is often simplier to derive. Nevertheless, if measures such as Arias intensity can be derived and assessed in relation to landslide frequency in Wenchuan and Northridge, it may be possible to adapt the method of **Kritikos et al. (2015)** to use such measures for estimating landslide hazard and subsequent exposure. Such an effort is likely to increase the utility of the landslide modelling and exposure methods described herein by allowing their direct application to various measure of earthquake ground shaking.

6. Conclusions

A road between South Westland district and Milford Sound via the Cascade and Hollyford River valleys has been considered since the 1870s, but recent legal decisions and a greater economic interest in tourism have resulted in renewed efforts to bring this concept to fruition.

This study has demonstrated a method for evaluating the exposure of planned transport links such as this to coseismic landsliding in earthquake scenarios for the purposes of informing decision-making. The method involves estimating the mean hazard values in close proximity to a proposed transport link from an underlying regional coseismic hazard map. The results for the HHH suggest that this route would have high exposure values, with particularly large values (>0.75) along 20-25% of the route. This road would be the most exposed link in the South Island State Highway network, and would increase the length of highly exposed road by 50-75% despite only increasing the total network length by 3%. As well as landsliding, the HHH would be exposed to surface rupture, ground shaking, lateral spreading, debris flow, and long-term river aggradation and flooding hazards. While financial exposure calculations have not been undertaken, given the high exposure values and length of road exposed, it is likely that repair costs for the HHH following an Alpine Fault earthquake would be substantial, potentially matching initial construction costs. The results herein demonstrate that vital information on hazard exposure of planned transport links can be developed, and should be derived from earthquake scenarios and landslide hazard maps.

7. Acknowledgements

The authors would like to thank Dr Theodosios Kritikos for his help and suggestions during the landslide hazard modelling, and Prof. Alex Densmore and Dr. Russell Blong whose helpful comments greatly improved the manuscript. We also thank the two anonymous reviewers for their helpful comments that helped focus the manuscript. This project was part funded by a University of Canterbury Doctoral Scholarship and the Mason Trust.

8. References

Archives New Zealand 2015. Part Roll 2/14 Plan of Cascade Pyke Valley Road (R22669314). Map/Plan. Christchurch Regional Office, New Zealand.

Barnes PM, Sutherland R, Delteil J 2005. Stike-slip structure and sedimentary basins of the southern Alpine Fault, Fiordland, New Zealand. Geological Society of America Bulletin, 117(3-4): 411-435.

Barnes PM, Bostock HC, Neil HL 2013. A 2300-year paleoearthquake record of the southern Alpine Fault and Fiordland Subduction Zone, New Zealand, based on stacked turbidites. Bulletin of the Seismological Society of America 103(4): 2424-2446, doi: 10.1785/0120120314.

Barth NC 2013a. The Cascade rock avalanche: implications of a very large Alpine Fault-triggered failure, New Zealand. Landslides 11(3): 327-341.

Barth NC 2013b. A Tectono-Geomorphic Study of the Alpine Fault, New Zealand (Thesis, Doctor of Philosophy). University of Otago. Retrieved from http://hdl.handle.net/10523/3847

Barth NC, Boulton C, Carpenter BM, Batt GE, Toy VG 2013. Slip localization on the southern Alpine Fault, New Zealand. Tectonics 31: 1–21, doi: 10.1002/tect.20041.

Barth NC, Kulhanek DK, Beu AG, Murray-Wallace CV, Hayward BW, Mildenhall DC, Lee DE 2014. New c. 270 kyr strike-slip and uplift rates for the southern Alpine Fault and implications for the New Zealand plate boundary. Journal of Structural Geology 64: 39-52, doi: 10.1016/j.jsg.2013.08.009.

Beavan J, Moore M, Pearson C 1999. Crustal deformation during 1994-1998 due to oblique continental collision in the central Southern Alps, New Zealand, and implications for seismic potential of the Alpine Fault. Journal of Geophysical Research 104: 233-255.

Beavan J, Denys P, Denham M, Hager B, Herring T, Molnar P 2010. Distribution of present-day vertical deformation across the Southern Alps, New Zealand, from 10 years of GPS data. Geophysical Research Letters 37: 7-11.

Berryman KR, Beanland S, Cooper AF, Cutten HN, Norris RJ, Wood PR 1992. The Alpine Fault, New Zealand: variation in Quaternary structural style and geomorphic expression. Annales tectonicae 6: 126-163.

Berryman KR, Cochran UA, Clark KJ, Biasi GP, Langridge RM, Villamor P 2012. Major earthquakes occur regularly on an isolated plate boundary fault. Science, 336(6089): 1690-1693.

Biasi GP, Langridge RM, Berryman KR, Clark KJ, Cochran U 2015. Maximum likelihood recurrence parameters and conditional probability of a ground-rupturing earthquake on the southern Alpine Fault, South Island, New Zealand. Bulletin of the Seismological Society of America 105(1): 94-107, doi: 10.1785/0120130259

Bird JF, Bommer JJ 2004. Earthquake losses due to ground failure. Engineering Geology 75: 147-179.

Boese CM, Townend TM, Smith E, Stern T 2012. Microseismicity and stress in the vicinity of the Alpine Fault, central Southern Alps, New Zealand. Journal of Geophysical Research: Solid Earth 117(B2), doi: 10.1029/2011JB008460.

Brunetti MT, Guzzetti F, Rossi M 2009. Probability distributions of landslide volumes. Nonlinear Processes in Geophysics 16:179-188.

Catani F, Casagli N, Ermini L, Righini G, Menduni G 2005. Landslide hazard and risk mapping at catchment scale in the Arno River basin. Landslides 24(4): 329-342.

Chevalier GG, Davies TRH, McSaveney MJ 2009. The prehistoric Mt Wilberg rock avalanche, Westland, New Zealand. Landslides 6: 253–262, doi: 10.1007/s10346-009-0156-5.

Chi W-C, Dreger D, Kaverina A 2001. Finite-source modeling of the 1999 Taiwan (Chi-Chi) Earthquake derived from a dense strong-motion network, Bulletin of the Seismological Society of America 91:1144–1157.

Chousianits K, Gaudio VD, Kalogeras I, Ganas A 2014. Predictive model of Arias intensity and Newmark displacement for regional scale evaluation of earthquake-induced landslide hazard in Greece. Soil Dynamics and Earthquake Engineering 65: 11-29.

Dadson SJ, Hovius N, Chen H et al. 2004. Earthquake-triggered increase in sediment delivery from an active mountain belt. Geology 32(8): 733-736, doi: 10.1130/G20639.1.

Davies TRH 1982. Spreading of rock avalanche debris be mechanical fluidization. Rock Mechanics 15(1): 9-24.

De Pascale GP, Langridge RM 2012. New on-fault evidence for a great earthquake in A.D. 1717, central Alpine Fault, New Zealand. Geology 40(9): 791-794, doi: 10.1130/G33363.1.

Dykstra JL 2012. The role of mass wasting and ice retreat on the post-LGM evolution of Milford Sound, Fiordland, New Zealand. Unpublished PhD Thesis, University of Canterbury, Christchurch, New Zealand 331p.

England K 2011. A GIS approach to landslide hazard management for the West Coast region, New Zealand. Unpublished MSc Thesis, University of Canterbury, Christchurch, New Zealand 210p.

ESRI 2015a. How IDW works. http://resources.arcgis.com/en/help/main/10.1/index.html#/How_IDW_works/009z00000075000000/ (accessed 3 September 2014).

ESRI 2015b. How flow accumulation works. http://resources.arcgis.com/en/help/main/10.1/index.html#/How_Flow_Accumulation_works/009z00000062000000/ (accessed 3 September 2014).

Field EH, Jordan TH, Cornell CA 2003. OpenSHA: A developing community-modelling environment for seismic hazard analysis. Seismological Research Letters 74(4): 406-419.

Giovinazzi S, Wilson T, Davis C et al. 2011. Lifelines performance and management following the 22 February 2011 Christchurch earthquake, New Zealand: Highlights for resilience. Bulletin of the New Zealand Society for Earthquake Engineering 44(4): 402-417.

GNS Active Faults Database n.d. http://data.gns.cri.nz/af/. Last Accessed: 5 June 2015.

Goff JR, Wells A, Chague-Goff C, Nichol SL, Devoy RJN 2004. The elusive AD 1826 tsunami, South Westland, New Zealand. New Zealand Geographer 60(2), 12p.

Goodwin P, Wright G 2001. Enhancing strategy evaluation in scenario planning: a role for decision analysis. Journal of Management Studies, 38(1): 1-16.

Gorum T, Fan X, van Western CJ et al. 2011. Distribution pattern of earthquake-induced landslides triggered by the 12 May 2008 Wenchuan earthquake. Geomorphology 133: 152-167.

Hancox GT, Perrin N 2009. Green Lake landslide and other giant and very large postglacial landslides in Fiordland, New Zealand. GNS Science Technical Report 93/18.

Howarth JD, Fitzsimmons SJ, Norris R, Jacobsen GE 2012. Lake sediments record cycles of sediment flux driven by large earthquakes on the Alpine Fault, New Zealand. Geology 40(12): 1091-1094.

Howarth JD, Fitzsimons SJ, Norris R, Jacobsen GE 2014. Lake sediments record high shaking that provides insights into the location and rupture length of large earthquakes on the Alpine Fault, New Zealand. Earth and Planetary Science Letters 403:340-351.

Hsü KJ 1975. Catastrophic debris streams (sturzstroms) generated by rockfalls. Geological Society of America Bulletin 86: 129-140.

Huang R, Pei X, Fan X, Zhang W, Li S, Li B 2012. The characteristics and failure mechanism of the largest landslide triggered by the Wenchuan earthquake, May 12, 2008, China. Landslides 9: 131-142, doi:10.1007/s10346-011-0276-6.

Hungr O, Corominas J, Eberhart E 2005. Estimating landslide motion mechanism, travel distance and velocity. In: Landslide risk management 99-128. Taylor & Francis Group, London.

Jibson RW 2007. Regression models for estimating coseismic landslide displacement. Engineering Geology 65: 209-218.

Keefer DK 1984. Landslides caused by earthquakes. Bulletin of the Geological Soceity of America 95: 406-421.

Kilburn CRJ, Sorenson S-A 1998. Runout lengths of sturzstroms: The control of initial conditions and of fragment dynamics. Journal of Geophysical Research 103(B8): 17877-17884.

Korup O 2004. Geomorphic implications of fault zone weakening: slope instability along the Alpine Fault, South Westland to Fiordland. New Zealand Journal of Geology and Geophysics 47: 257-267.

Korup O 2005a. Geomorphic hazard assessment of landslide dams in South Westland, New Zealand: fundamental problems and approaches. Geomorphology 66: 167-188, doi: 10.1016/j.geomorph.2004.09.013.

Korup O 2005b. Distribution of landslides in southwest New Zealand. Landslides: 2:43-51, doi: 10.1007/s10346-004-0042-0.

Korup O 2005c. Large landslides and their effect on sediment flux in South Westland, New Zealand. Earth Surface Processes and Landforms 30: 305-323, doi: 10.1002/esp.1143.

Kritikos T, Robinson TR, Davies TRH 2015. Regional coseismic landslide hazard assessment without historical landslide inventories: a new approach. Journal of Geophysical Research: Earth Surface

Lee CT 2014. Statistical seismic landslide hazard analysis: An example from Taiwan. Engineering Geology 182: 201-212.

Legros F 2002. The mobility of long-runout landslides. Engineering Geology 63(3): 301-331.

Leitner B, Eberhart-Phillips D, Anderson H, Nabelek JL 2001. A focused look at the Alpine Fault, New Zealand: Seismicity, focal mechanisms, and stress observations. Journal of Geophysics Research 106(B2): 2193-2220.

McCahon I, Elms D, Dewhirst R 2006. Alpine Fault earthquake scenario. West Coast Regional Lifelines Group Technical Report. 204p.

Montibeller G, Gummer H, Tumidei D 2006. Combining scenario planning and multi-criteria decision analysis in practice. Journal of Multi-Criteria Decision Analysis, 14(1-3): 5-20.

New Zealand Map Series 10 1966. Sheet 28. Land Information New Zealand.

Nicoletti PG, Sorriso-Valvo M 1991. Geomorphic controls of the shape and mobility of rock avalanches. Geological Society of America Bulletin 103:1365-1373.

Norris RJ, Cooper AF 2001. Origin of small-scale segmentation and transpressional thrusting along the Alpine Fault, New Zealand. Geological Society of America Bulletin 107: 231-240, doi: 10.1130/0016-7606(1995)107<0231.

Okada Y, Ochiai H, Kurokawa U, Ogawa Y, Asano S 2008. A channelized long run-out debris slide triggered by the Noto Hanto Earthquake in 2007, Japan. Landslides 5(2): 235-239.

Oldfield S 2012. Assessment of access options for Milford Sound. Environment Southland, Invercargill, New Zealand. 65p.

Otago Daily Times 2014. A Haast-Hollyford Road. http://www.odt.co.nz/opinion/editorial/297509/haast-hollyford-road (accessed 5 February 2015).

Otago Daily Times 2015. Next step towards highway. http://www.odt.co.nz/regions/west-coast/330985/next-step-towards-highway (accessed 5 February 2015).

Paterson BR 1996. Slope instability along State Highway 73 through Arthur's Pass, South Island, New Zealand. New Zealand Journal of Geology and Geophysics, 39(3): 339-350.

Pellicani R, van Western CJ, Spilotro G 2014. Assessing landslide exposure in areas with limited landslide information. Landslides 11(3): 463-480, doi: 10.1007/s10346-013-0386-4.

Robinson TR 2014. Assessment of coseismic landsliding from an Alpine Fault earthquake scenario, New Zealand. Unpublished PhD Thesis, University of Canterbury, Christchurch, New Zealand, 293p.

Robinson TR, Davies TRH 2013. Review article: Potential geomorphic consequences of a future great (M_w=8.0+) Alpine Fault earthquake, South Island, New Zealand. Natural Hazards and Earth System Sciences 13:2279-2299, doi: 10.5194/nhess-13-2279-2013.

Robinson TR, Davies TRH, Reznichenko NV, De Pascale GP 2014. The extremely long-runout Komansu rock avalanche in the Trans Alai range, Pamir Mountains, southern Kyrgyzstan. Landslides, doi: 10.1007/s10346-014-0492-y.

Scheidegger AE 1973. On the prediction of the reach and velocity of catastrophic landslides. Rock Mechanics 5: 231-236.

Schoemaker PJ 1993. Strategic decisions in organizations: rational and behavioural views. Journal of management studies 30(1): 107-129.

Schroeder MJ, Lambert JH 2011. Scenario-based multiple criteria analysis for infrastructure policy impacts and planning. Journal of Risk Research 14(2): 191-214.

Stark CP, Guzzetti F 2009. Landslide rupture and the probability distribution of mobilized debris volumes. Journal of Geophysical Research: Earth Surface, 114(F2).

Stirling M, McVerry G, Gerstenberger M et al. 2012. National seismic hazard model for New Zealand: 2010 update. Bulletin of the Seismological Society of America, 102(4): 1514-1542.

Sutherland R, Eberhart-Phillips D, Harris RA et al. 2007. Di Great earthquakes occur on the Alpine Fault in central South Island, New Zealand? Geophysical Monologue Series 175: 235-251.

The New Zealand Herald 2010. A highway through heritage. http://www.nzherald.co.nz/nz/news/article.cfm?c_id=1&objectid=10627334 (accessed 5 February 2015).

The Press 2014. http://www.stuff.co.nz/the-press/news/west-coast/9872211/230m-Haast-Hollyford-road-mooted (accessed 5 February 2015).

Wells A, Yetton MD, Duncan RP, Stewart GH 1999. Prehistoric dates of the most recent Alpine Fault earthquakes, New Zealand. Geology 27(11): 995-998.

Wells DL, Duncan RP, Stewart GH 2001. Forest dynamics in Westland, New Zealand: the importance of large, infrequent earthquake-induced disturbance. Journal of Ecology, 89: 1006-1018.

Wells A, Goff J 2007. Coastal dunes in Westland, New Zealand, provide a record of paleoseismic activity on the Alpine Fault. Geology 35(8):731-734, doi: 10.1130/G23554A.1.

Wilderness Magazine 2014. http://www.wildernessmag.co.nz/view/page/articles/read/haast-hollyford-road-could-go-to-court/ (accessed 5 February 2015).

Xu Q, Zhang S, Li WL, van Asch TWJ 2012 The 13 August 2010 catastrophic debris flows after the 2008 Wenchuan earthquake, China. Natural Hazards and Earth System Sciences 12:201-216.

Yetton MD 1998. Progress in understanding the paleoseismicity of the central and northern Alpine Fault, Westland, New Zealand. New Zealand Journal of Geology and Geophysics 41:475-483.

Yu S, Chen H, Kuo L 1997. Velocity field of GPS stations in the Taiwan area, Tectonophysics, 274(1):41–59.

Zhang J, He L 2002. Geology of Taiwan Province. Geology of China. Geological Publishing House. ISBN 7-116-02268-6.

Tables:

Table 1 Data used for modelling isoseismals for an Alpine Fault earthquake in OpenSHA.

[a] Chosen to be close to the maximum measured uplift rate where stresses are assumed to be highest (**Norris and Cooper, 2001**).

[b] Rake is measured relative to fault strike, rather than as absolute strike, with 0° representing sinistral and 180° representing dextral movement; positive values signify reverse motion (**Field et al., 2003**).

[c] Two different fault dips are used for the central and northern section, and the southern section, reflecting known changes in the fault parameters between these two sections (see **Barth et al., 2013**).

Data Type	**Input Data**	**Reference**
	Intensity Measure Relationships	
Intensity Measure Type	MMI	
Tectonic Region	Active Shallow Crust	
Component	Average Horizontal	
	Site Data Providers	
Vs30 (m/sec)	180.0 (Default)	
Site Data Provider	Global Vs30	
Digital Elevation Model	SRTM30 Version 2	
Region Type	Active Tectonic	
	Earthquake Rupture	
Rupture Type	Finite source	
Magnitude	8.0	See text
Epicentre[a]	43.50S, 170.12E[a]	
Rake[b]	172°	**Barth et al., 2013**
Fault Dip[c]	60°SE and 82°SE	**Barth et al., 2013**
Fault Depth	12 km	**Beavan et al., 1999, 2010**
Fault tips	44.51S, 167.83E 42.73S, 171.43E	
Fault slip rate	~38 mm/a	

Figures:

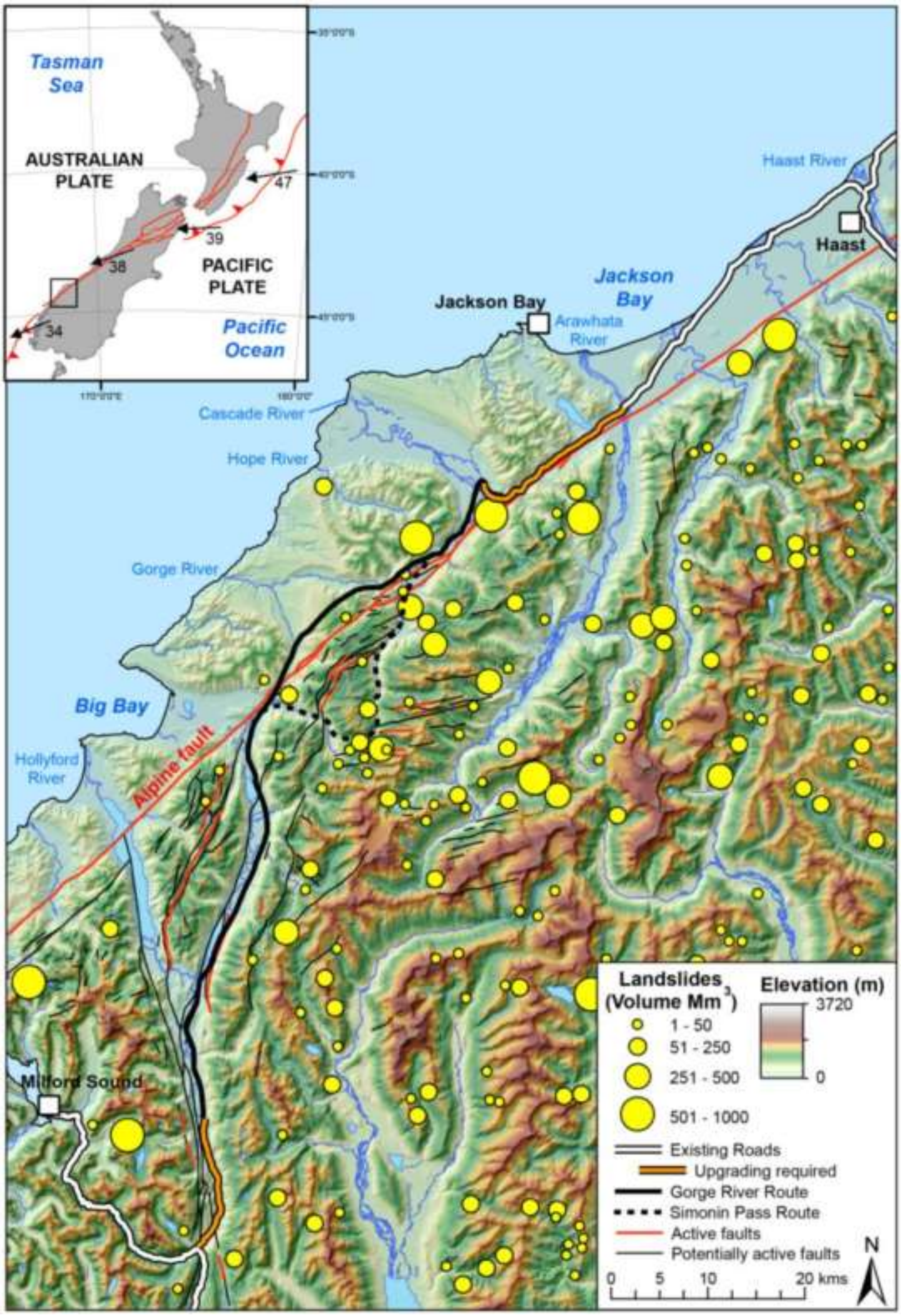

Figure 1 Location of the proposed Haast-Hollyford Highway showing both potential routes via Simonin Pass and Gorge River in relation to mapped active faults and identified large (>1

million m^3) landslides. Landslide volumes after **Korup (2004)**, **Korup (2005a, b, c)**, **Hancox and Perrin (2009)**, **Barth (2013a, b), and include new interpretations by this study**. Faults after the GNS Science active fault database (http://data.gns.cri.nz/af/) and Barth et al. (2013). Inset – Tectonic setting of New Zealand showing plate boundary faults. Plate motion vectors in mm/a.

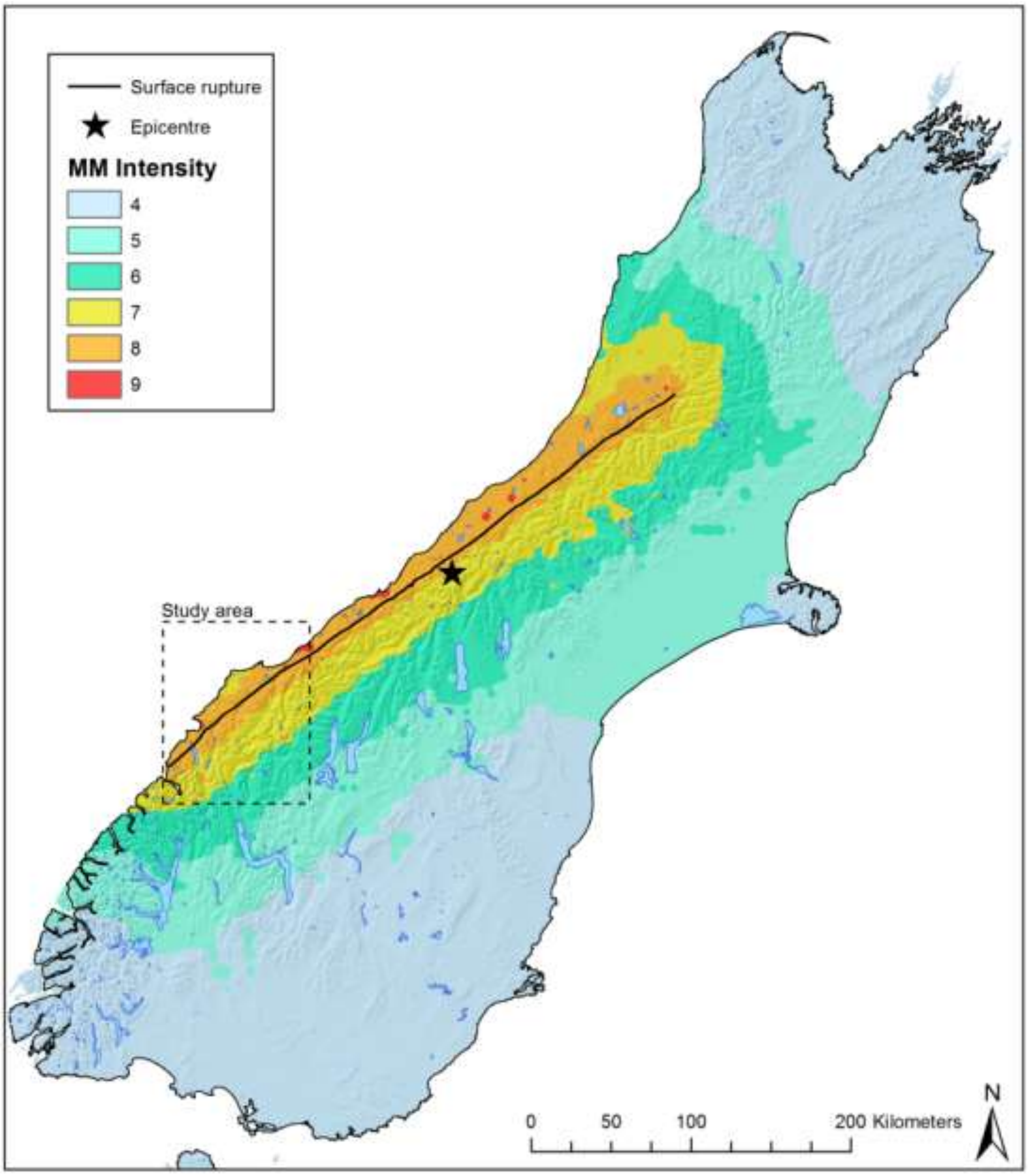

Figure 2 Modelled isoseismals for an M_w8.0 Alpine Fault earthquake with 380 km fault rupture. See **Table 1** for modelling data.

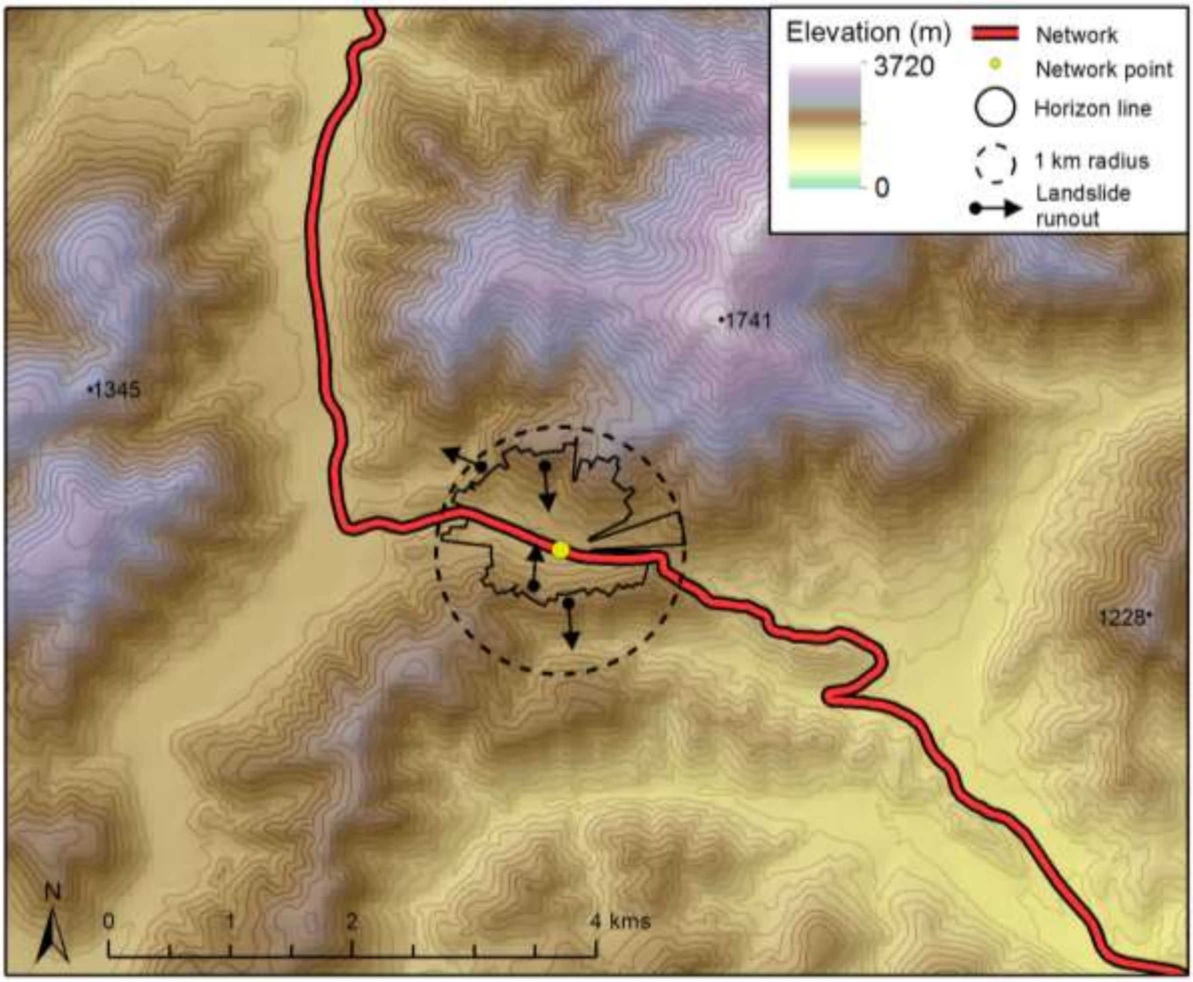

Figure 3 Schematic diagram showing the area contributing landslide hazard values for estimating exposure. Cells within the horizon line (solid black line) are located on slopes facing the network and landslide runout paths are inferred to be towards the network. Those cells outside the horizon line have runout paths away from the network, in this case on opposing sides of the ridgeline.

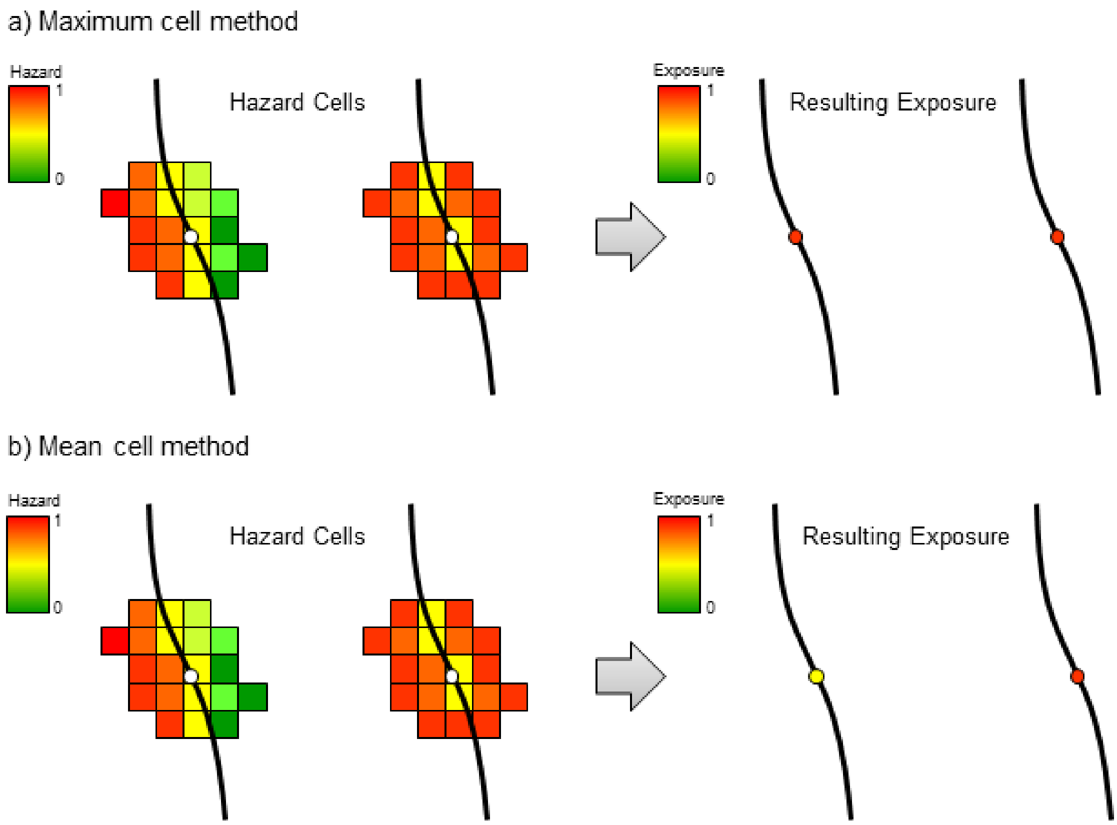

Figure 4 Schematic diagram comparing the resulting exposure for a point on a network using a) the maximum observed hazard value, and b) the mean hazard values of all cells. Note the reduced exposure from a to b for the point with large hazard values on one side only (i.e. a range-front section of the network) compared to the point with large hazard values on all sides (i.e. a section within the mountains).

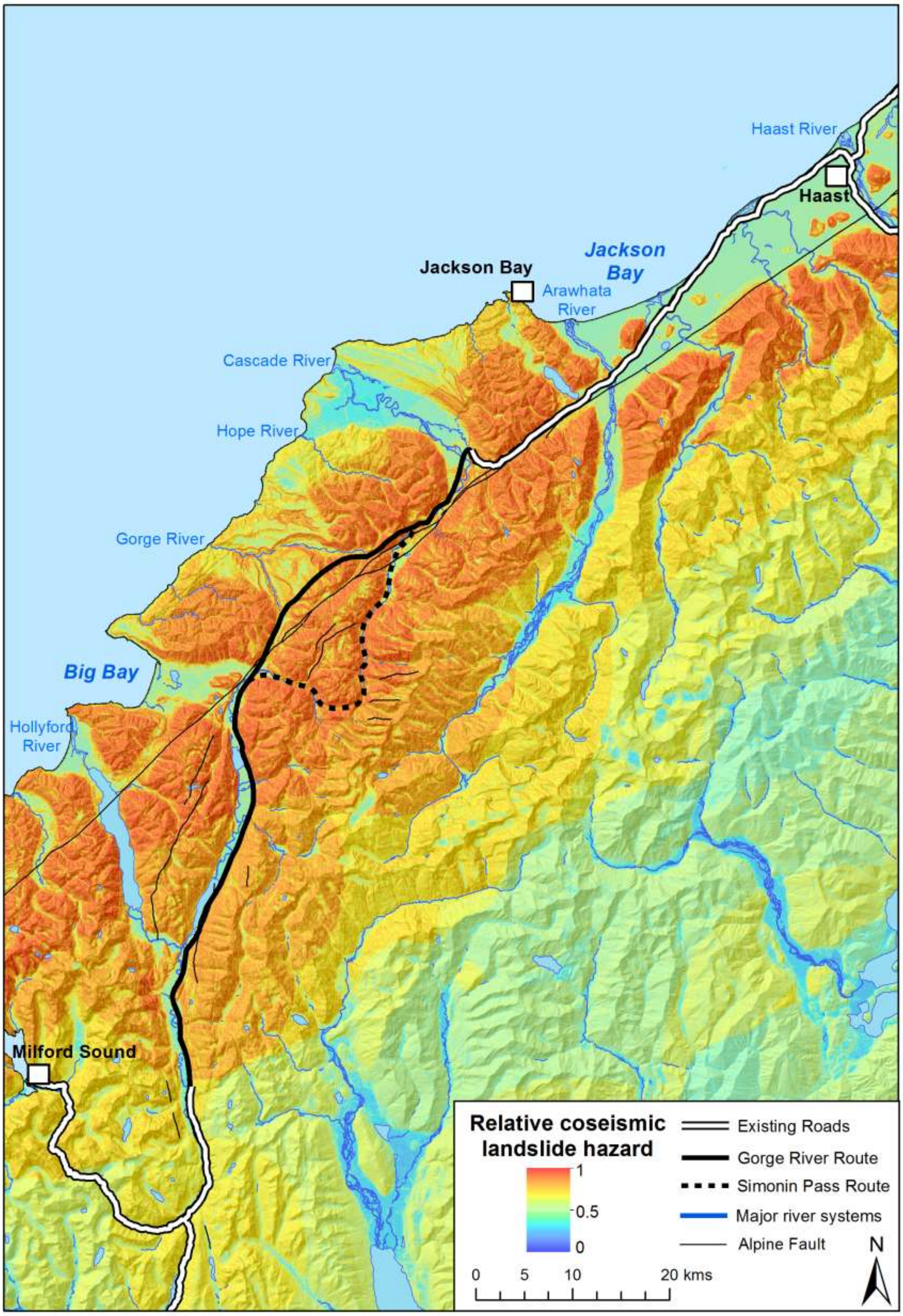

Figure 5 Coseismic landslide hazard (in terms of relative probability) in the study area from an M_w8.0 Alpine Fault earthquake.

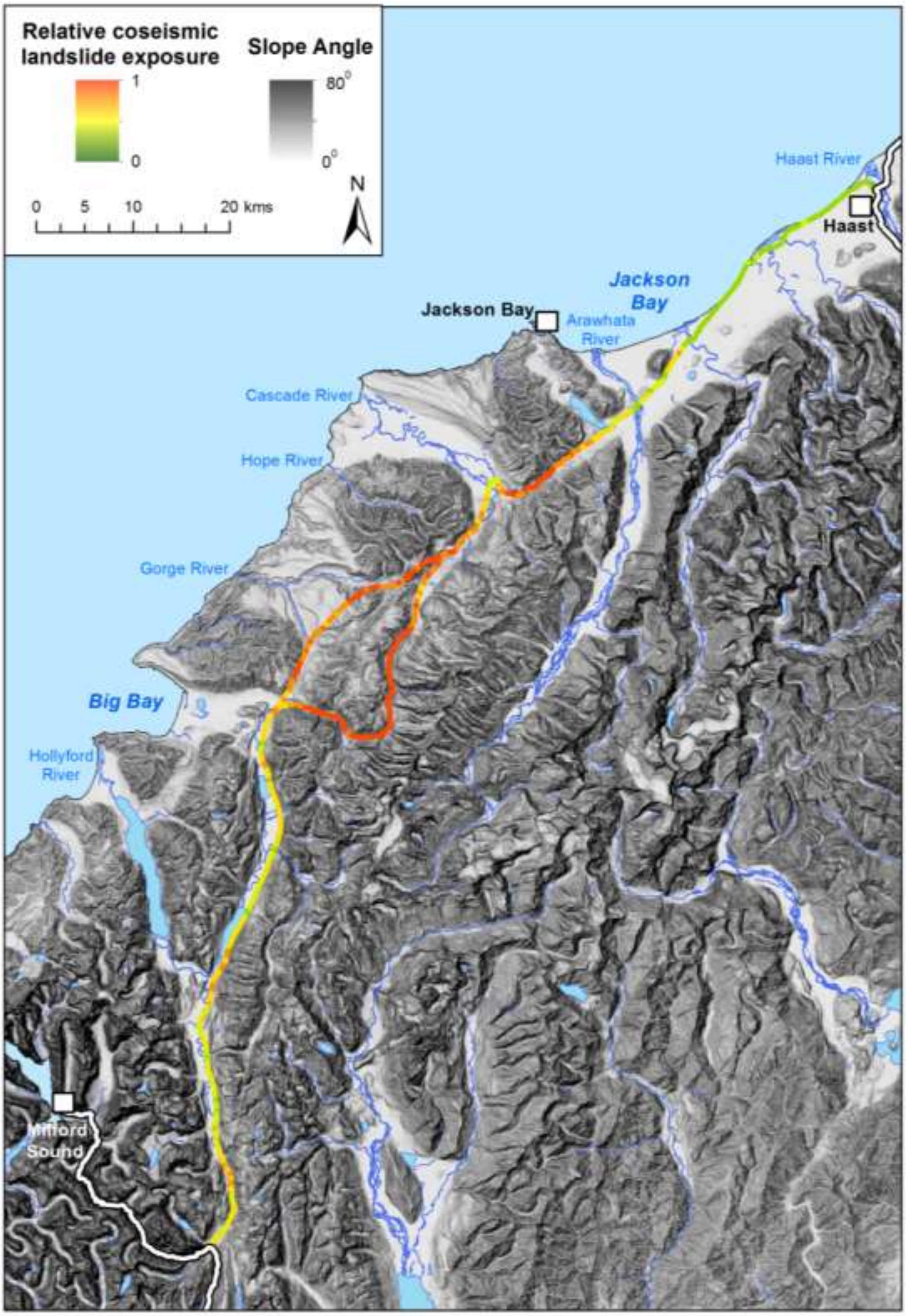

Figure 6 Relative coseismic landslide exposure of the Gorge River and Simonin Pass routes of the proposed Haast-Hollyford Highway for an Alpine Fault earthquake.

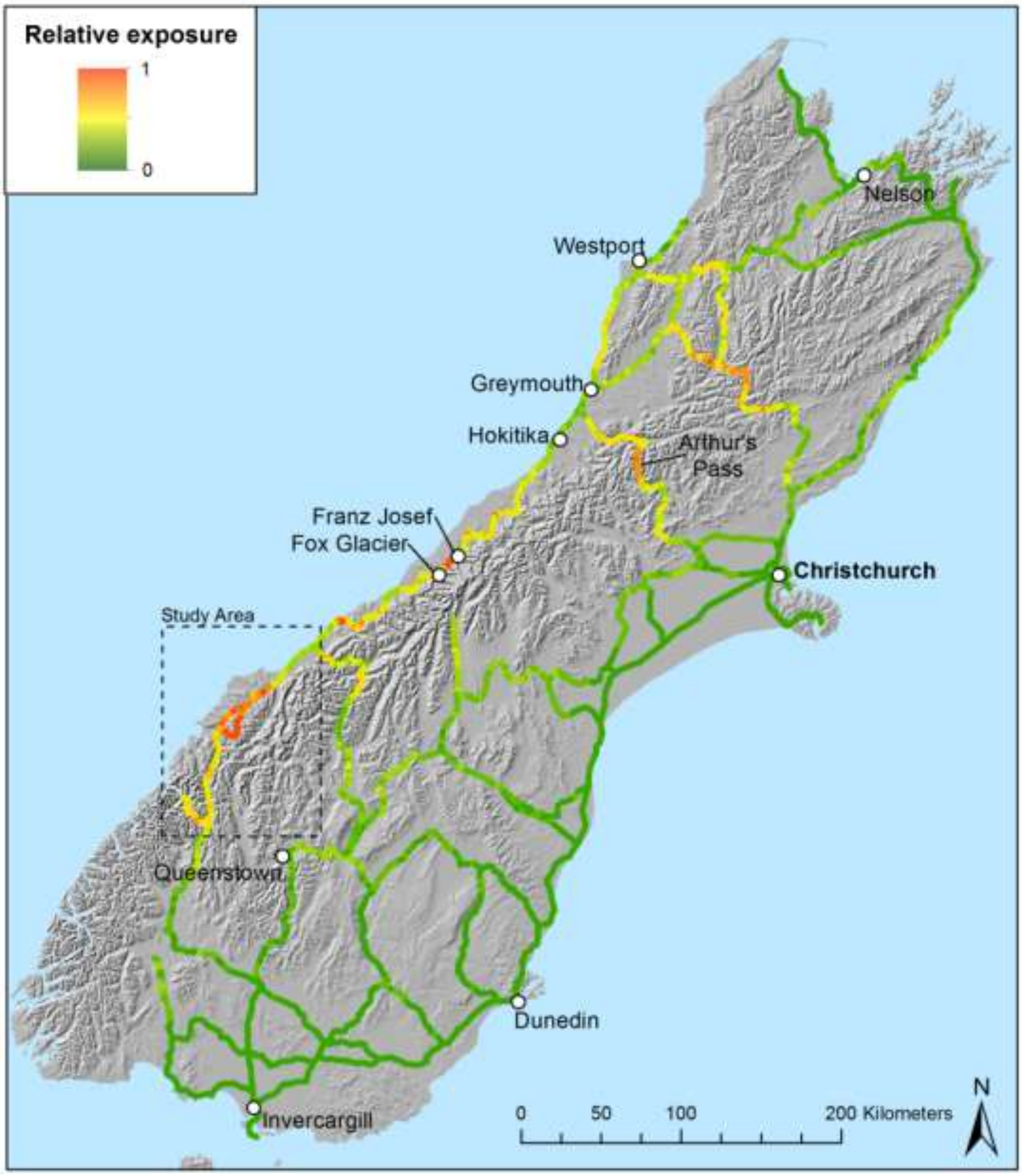

Figure 7 Relative coseismic landslide exposure for the current South Island State Highway network for an Alpine Fault earthquake.